

# Chandra observations of ten galaxy clusters

*Iu. Babyk*<sup>1\*</sup>, *O. Melnyk*<sup>2,3</sup>, *A. Elyiv*<sup>1,3</sup>

<sup>1</sup>Main Astronomical Observatory of the National Academy of Sciences of Ukraine, Zabolotnoho 27, 03680, Kyiv, Ukraine

<sup>2</sup>Astronomical Observatory, Taras Shevchenko National University of Kyiv, Observatorna str., 4, 04053, Kyiv, Ukraine

<sup>3</sup>Institut d'Astrophysique et de Géophysique, Université de Liège, 4000, Belgium

In the present study the X-ray properties of 10 galaxy clusters (CL0024+17, RXJ1347.5+1145, A223, A521, A611, A697, A907, A1204, A1413 and A2744) are analysed using the archival X-ray data of the Chandra observatory. The average temperature of each cluster is estimated to be  $\sim 4 - 10$  keV, and the radial temperature profiles are reconstructed. Using the Navarro-Frenk-White (NFW) density profile of the dark matter the density and mass profiles for the dark matter and the hot diffuse gas, and also the total mass profiles are derived. The typical size of galaxy clusters and the density of the dark matter halo are estimated to be  $\sim 0.1 - 2$  Mpc and  $\sim 10^{-22} - 10^{-24}$  kg/m<sup>3</sup>, respectively. The fraction of each component in the total cluster mass for the whole sample is found to be  $\sim 80-90\%$  for dark matter and  $\sim 10 - 20\%$  for intracluster gas, respectively.

**Key words:** galaxies: clusters: general – intergalactic medium – X-rays

## INTRODUCTION

The galaxy clusters are the largest gravitationally bound systems in the Universe. The main targets of their study are the cluster evolution, the structure formation and the cluster population [1]. The mass of the cluster is an important characteristic for defining the cosmological parameters. The observations of the hot gas in X-rays are very useful and effective tool for the precise estimation of the total mass [2, 9]. The present generation of satellites such as the XMM-Newton and Chandra represent a giant step forward in terms of resolution and sensitivity of X-ray observations. So using the assumption of the hydrostatic equilibrium one can precisely reconstruct the total mass distribution in clusters [6]. Therefore the main aim of the present study is to derive the total mass profiles of 10 galaxy clusters and to check the correspondence of their shapes. We also report about the estimations of temperature, density and mass of these galaxy clusters. Throughout the paper we assume  $H_0 = 73$  km/s/Mpc,  $\Omega_m = 0.27$  and  $\Omega_\Lambda = 0.73$ .

## DATA PROCESSING

Our sample contains ten galaxy clusters with  $z < 0.5$ . The main characteristics of the clusters are presented in Table 1. The first step of the data reduction was done with the CIAO software package version 4.2. We split the image of each cluster on the concentric rings toward from the centre, generated ARF and RMF files using the SPEXTRACT subroutine, and derived the spectrum in each ring for each cluster. Then we used the Xspec software package version 12.6 for the spectra fitting. We applied

the WABS\*MEKAL model, where WABS is the Galactic absorption parameter for the cluster [3] and MEKAL is a model which describes a diffuse emission from the hot plasma.

We extracted the temperature in each region and parameter Norm from the MEKAL model, which is proportional to the electron and proton concentrations, within the energy range 0.4 – 7.0 keV [7]. All other parameters of the model, for example, metallicity (we used the solar value  $Z = 0.3$ ), redshift and WABS were frozen. The average values of the temperature are shown in Table 1. We also estimated the flux of each cluster.

## METHOD

We assume that the gas temperature is constant along the radius and is in hydrostatic equilibrium with cluster potential [5, 8]. We run numerical simulations using the NFW density profile of the dark matter [4] for reconstruction of the parameters of the dark matter distribution in each cluster. The NFW profile can be presented as:

$$\rho_{DM}(r) = \frac{\rho_0}{(r/r_s)(1+r/r_s)^2}, \quad (1)$$

where  $r_s$  is the characteristic scale radius of the halo and  $\rho_0$  is the typical density. The integrated mass of the dark matter inside the radius  $r$  is:

$$M(< r) = \int_0^r 4\pi r^2 \rho(r) dr = 4\pi \rho_0 r_s^3 \left[ \ln\left(\frac{r_s + r}{r_s}\right) + \frac{r}{r_s + r} \right]. \quad (2)$$

\*babikyura@gmail.com

Table 1: The main characteristics of the sample.

Cluster	ObsID	$z$	Detector	Exp.time (ks)	$N_H$ , $10^{20}\text{cm}^2$	$T$ , keV	Flux, $10^{-13}\text{erg/cm}^2/\text{s}$
A223	4967	0.21	ACIS-I	45.6	2.2	$5.01^{+0.85}_{-0.91}$	2.83
A521	430	0.25	ACIS-S	39.6	5.81	$10.21^{+1.85}_{-1.91}$	4.25
A611	3194	0.28	ACIS-S	36.6	4.99	$6.24^{+0.78}_{-0.67}$	1.13
A697	4217	0.28	ACIS-I	19.7	3.42	$10.22^{+1.24}_{-1.55}$	6.6
A907	3205	0.15	ACIS-I	47.7	5.4	$5.81^{+0.75}_{-0.66}$	7.59
A1204	2205	0.17	ACIS-I	23.9	1.4	$4.84^{+1.93}_{-1.34}$	2.28
A1413	537	0.14	ACIS-I	9.34	2.19	$8.07^{+2.28}_{-2.02}$	4.96
A2744	2212	0.31	ACIS-S	25.14	1.62	$9.82^{+0.43}_{-0.41}$	6.14
CL0024	929	0.39	ACIS-S	40.34	4.22	$4.35^{+0.51}_{-0.44}$	0.22
RXJ1347	2222	0.45	ACIS-S	93.9	4.85	$11.81^{+1.89}_{-2.04}$	8.05

Massive dark matter halo possesses the field of gravitational potential which forms the shape of the hot gas halo. Gravitational potential  $\varphi$  can be found from the following relation:

$$\frac{d\varphi}{dr} = G \frac{M(< r)}{r^2}. \quad (3)$$

Using the hydrostatic equilibrium of the X-ray emitting gas with the cluster potential and NFW dark matter profile, we derived and solved equation for unknown gas density distribution:

$$\frac{\nabla \rho_g}{\rho_g} = -\nabla \varphi(r) \frac{\mu m_p}{k T_g}. \quad (4)$$

### SURFACE BRIGHTNESS PROFILE

Using  $r_s$  and  $\rho_0$  parameters we determined the cluster potential and the hot gas distribution profile. We also used these parameters to derive the surface brightness profiles (see Fig. 1), which were then compared to the observed ones.

In Fig. 1 the surface brightness profile for CL0024+17 cluster is present as an example. The surface brightness profiles for other clusters from our sample have similar shapes but different values of  $r_s$  and  $\rho_0$ . These values vary from 0.1 to 2 Mpc for parameters  $r_s$  and  $10^{-22}$ - $10^{-24}$  kg/m<sup>3</sup> for  $\rho_0$ .

### RESULTS OF THE MODELLING

The integrated total mass profiles for the whole sample of the galaxy clusters as well as the scaled mass profiles for these clusters are shown in Fig. 2. The masses are scaled to  $M_{200}$  and the radii to  $R_{200}$

( $R_{200}$  is the radius where the density is equal to  $200\rho_{cr}$  at the cluster redshift and  $M_{200}$  is the mass within this radius,  $\rho_{cr}$  is the critical density of the Universe). In Table 2 the cluster parameters obtained from the modelling are presented.

### CONCLUSIONS

We reconstructed the total mass density profiles of ten galaxy clusters using the Chandra observations. Our sample has the temperature within the range from 4 to 10 keV and covers an order of magnitude range in mass from  $M_{200} = 3.1 \times 10^{14} M_\odot$  to  $2.2 \times 10^{15} M_\odot$ . We confirm that the NFW profile represents the observed mass profiles quite well. The dark matter fraction in the total mass of the clusters is found to be 71-91%.

### REFERENCES

- [1] Arnaud M., Pratt G. W. & Pointecouteau E. 2004, *Memorie della Societa Astronomica Italiana*, 75, 529
- [2] Coia D., McBreen B., Metcalfe L. et al. 2005, *A&A*, 431, 433
- [3] Dickey J. M. & Lockman F. J. 1990, *ARA&A*, 28, 215
- [4] Navarro J. F., Frenk C. S. & White S. D. M. 1996, *ApJ*, 462, 563
- [5] Pointecouteau E., Arnaud M. & Pratt G. W. 2005, *Advances in Space Research*, 36, 659
- [6] Pratt G. W. & Arnaud M. 2005, *A&A*, 429, 791
- [7] Vikhlinin A., Forman W. & Jones C. 1999, *ApJ*, 525, 47
- [8] Vikhlinin A., Kravtsov A., Forman W. et al. 2006, *ApJ*, 640, 691
- [9] Zhang Y.-Y., Finoguenov A., Böhringer H. et al. 2004, *A&A*, 413, 49

Table 2: The cluster parameters obtained from the modelling.

Cluster	$R_{200}$ Mpc	$M_{tot,200}$ $10^{14}M_{\odot}$	$M_{DM,200}$ $10^{14}M_{\odot}$	$M_{g,200}$ $10^{13}M_{\odot}$	$M_{DM,200}/M_{tot,200}$
A223	$1.44^{+0.26}_{-0.21}$	$4.44^{+0.45}_{-0.61}$	$3.79^{+0.51}_{-0.34}$	$6.26^{+0.81}_{-0.45}$	0.85
A521	$1.67^{+0.16}_{-0.12}$	$3.14^{+0.83}_{-0.73}$	$2.87^{+0.27}_{-0.16}$	$2.61^{+0.36}_{-0.45}$	0.91
A611	$1.44^{+0.19}_{-0.15}$	$4.98^{+0.12}_{-0.23}$	$3.57^{+0.09}_{-0.12}$	$1.41^{+0.06}_{-0.07}$	0.72
A697	$2.04^{+0.19}_{-0.22}$	$13.71^{+1.46}_{-1.34}$	$10.66^{+0.54}_{-0.43}$	$30.45^{+1.73}_{-1.61}$	0.77
A907	$1.67^{+0.15}_{-0.21}$	$6.67^{+0.54}_{-0.65}$	$5.95^{+0.20}_{-0.25}$	$7.56^{+0.42}_{-0.32}$	0.89
A1204	$1.28^{+0.44}_{-0.26}$	$3.05^{+0.33}_{-0.23}$	$2.54^{+0.15}_{-0.12}$	$5.01^{+0.74}_{-0.70}$	0.83
A1413	$1.83^{+0.66}_{-0.57}$	$8.61^{+0.46}_{-0.49}$	$7.23^{+0.65}_{-0.71}$	$14.81^{+1.10}_{-0.91}$	0.84
A2744	$2.38^{+0.36}_{-0.31}$	$22.26^{+1.30}_{-1.20}$	$18.81^{+1.80}_{-2.10}$	$33.11^{+1.72}_{-2.51}$	0.84
CL0024	$1.24^{+0.12}_{-0.17}$	$3.51^{+0.38}_{-0.47}$	$3.09^{+0.37}_{-0.33}$	$4.56^{+0.86}_{-0.49}$	0.88
RXJ1347	$1.85^{+0.16}_{-0.18}$	$12.22^{+1.93}_{-1.75}$	$8.75^{+0.24}_{-0.24}$	$34.91^{+1.08}_{-1.23}$	0.71

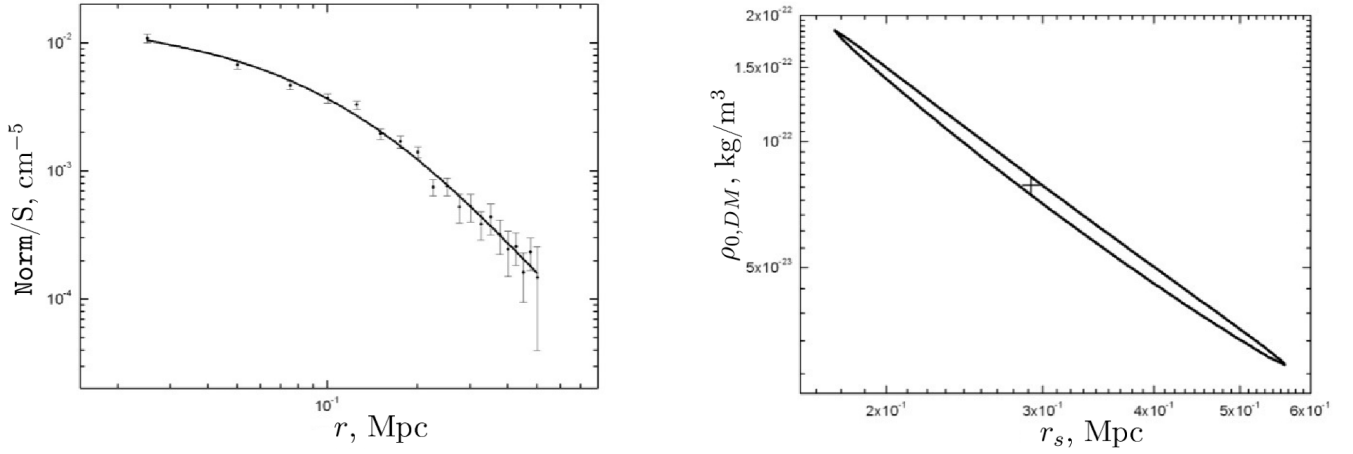


Fig. 1: Left: The observed (points with bars) and simulated surface brightness profile (solid line) of CL0024+17. The bars represent the  $2\sigma$  deviation. Right: The area values of  $r_s$  and  $\rho_0$  with 90% probability. The lowest value of  $\chi^2$  is marked by the cross (the best-fit of observational surface profile).

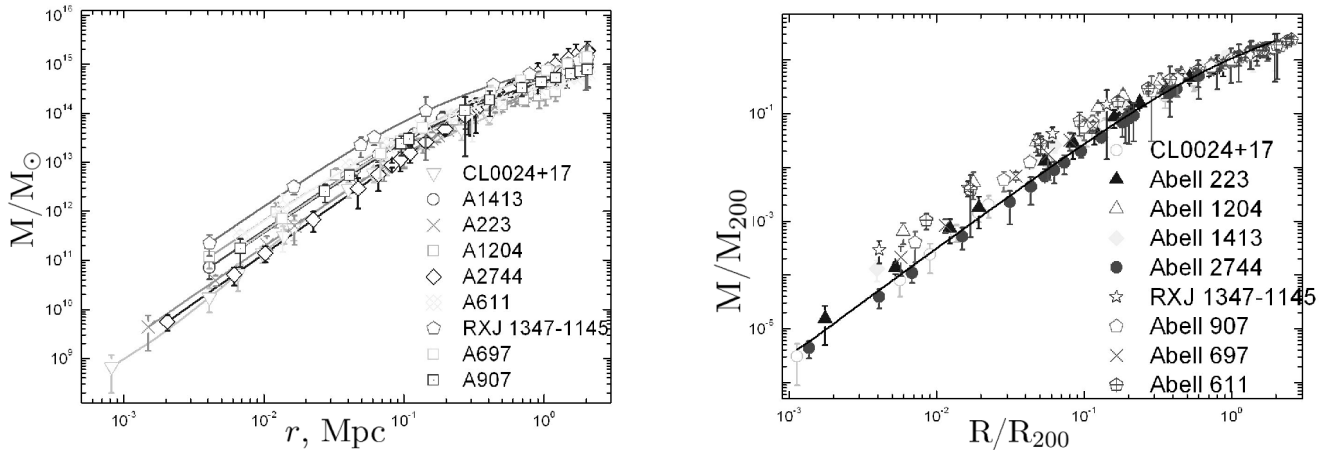


Fig. 2: Left: The total mass profiles. The solid lines is the best-fit of the NFW model. Right: The scaled mass profiles. The solid line represents the mean scaled NFW profile.